

SGLT-1-mediated glucose uptake protects intestinal epithelial cells against LPS-induced apoptosis and barrier defects: a novel cellular rescue mechanism?

Linda C. H. Yu,* Andrew N. Flynn,* Jerrold R. Turner,[†] and Andre G. Buret*¹

*Department of Biological Sciences, Mucosal Inflammation Research Group, University of Calgary, Calgary, AB, Canada; and [†]Department of Pathology, University of Chicago, Chicago, Illinois, USA

ABSTRACT Excessive apoptosis induced by enteric microbes leads to epithelial barrier defects. This mechanism has been implicated in the pathogenesis of inflammatory bowel diseases (IBD) and bacterial enteritis. The sodium-dependent glucose cotransporter (SGLT-1) is responsible for active glucose uptake in enterocytes. The aim was to investigate the effects of SGLT-1 glucose uptake on enterocyte apoptosis and barrier defects induced by bacterial lipopolysaccharide (LPS). SGLT-1-transfected Caco-2 cells were treated with LPS (50 $\mu\text{g}/\text{mL}$) in low (5 mM) or high (25 mM) glucose media. LPS in low glucose induced caspase-3 cleavage, DNA fragmentation, and increased paracellular permeability to dextran in epithelial cells. These phenomena were significantly attenuated in high glucose. LPS increased SGLT-1 activity in high, but not low glucose media. Addition of phloridzin, which competitively binds to SGLT-1, inhibited the cytoprotection mediated by high glucose. Western blot showed that LPS in high glucose increased the levels of anti-apoptotic Bcl-2 and Bcl-X_L, and did not change proapoptotic Bax. Differential extraction of membranous vs. cytosolic cell components demonstrated that high glucose inhibits mitochondrial cytochrome *c* translocation to cytosol. Collectively, SGLT-1-mediated glucose uptake increases anti-apoptotic proteins, and protects enterocytes from LPS-induced apoptosis and barrier defects. The understanding of this novel glucose-mediated rescue mechanism may lead to therapeutic interventions for various enteric diseases. *FASEB J.* 19, 1822–1835 (2005)

Key Words: enterocytes apoptosis • paracellular permeability • LPS • SGLT-1 • glucose

INTESTINAL EPITHELIAL CELLS and their tight junctions act as a barrier against the penetration of luminal microbial pathogens, cytotoxic agents, and other intestinal contents. Physiological extrusion of enterocytes via apoptosis does not compromise this barrier functions (1). In contrast, in a variety of circumstances, including exposure to enteric pathogens (e.g., *Giardia duodenalis*, *Escherichia coli*, *Salmonella enteritica*, and *Helicobacter pylori*) (2–6), cytotoxic agents (e.g., wheat

gliadin, tumor suppressive drugs, and radiation) (7, 8), or host immune factors (e.g., cytotoxic T cells, TNF α , and Fas/FasL) (9–11), augmented enterocyte apoptosis may increase epithelial paracellular permeability and hence breach intestinal barrier function. Cytoprotective mechanisms evolved by enterocytes represent the corner stone of cell survival and homeostasis upon exposure to pathological proapoptotic stimuli.

Cells that undergo apoptosis (programmed cell death) display morphological changes, e.g., cell shrinkage, membrane blebbing, mitochondrial swelling, and chromatin condensation. Apoptosis may be initiated extrinsically via Fas or TNF receptors, or intrinsically via mitochondrial pathways, which are mediated by caspase-8 and caspase-9 respectively. Both pathways lead to caspase-3 cleavage and ultimately endonuclease activation and nuclear DNA fragmentation (see reviews) (12). Caspase-8-dependent signaling may activate caspase-3 via mitochondrial-dependent or -independent mechanisms. The family of Bcl-2 proteins (e.g., anti-apoptotic Bcl-2, Bcl-X_L, and proapoptotic Bax) are important regulators of mitochondrial-dependent apoptosis (13). These Bcl-2-related proteins target the mitochondrial outer membrane voltage-dependent anion channel (VDAC) and either modulate its expression or change its conformation to alter membrane potential (14, 15). Upon proapoptotic signaling, VDAC in conjunction with proteins like Bax are responsible for the loss of membrane potential and the release of cytochrome *c* into the cytosol, where it forms apoptosomes to activate caspase-9 (14, 15). Anti-apoptotic Bcl-2 and Bcl-X_L proteins are potent inhibitors of this mitochondrial-mediated cell death pathway (14, 15).

Apoptosis is an energy-dependent process (16). The major sources of energy production in cells are metabolic processes of glycolysis and mitochondrial oxidative phosphorylation of glucose derivatives. Previous reports have demonstrated that blockage of glycolysis and energy production with 2-deoxyglucose prevents

¹ Correspondence: Department of Biological Sciences, BI 117, Mucosal Inflammation Research Group, University of Calgary, 2500 University Dr. N.W., Calgary, AB T2N 1N4, Canada. E-mail: aburet@ucalgary.ca
doi: 10.1096/fj.05-4226com

cytotoxic doxorubicin-induced apoptosis in enterocytes (17). Intracellular high glucose level protects cardiac myocytes and vascular smooth muscle cells from apoptosis in hypoxic ischemia and balloon distension injury (18, 19). In T cell hypoxia-induced apoptosis, high intracellular glucose concentration switches proapoptotic signals from caspase-8 to caspase-9-dependent pathways (20). However, the effects of active sugar uptake on epithelial cell apoptosis remain unknown.

The main apical transporter for active glucose uptake in small intestinal epithelial cells is the sodium-dependent glucose cotransporter (SGLT) -1 (21). The different types of membrane-associated glucose transporters include three members of SGLT and fourteen members of GLUT transporters (22). SGLT-1 unidirectionally mediates glucose absorption from the intestinal lumen into epithelial cells. The basolateral transporter GLUT-2 facilitates diffusive transport of intracellular glucose into the interstitium and bloodstream (23). SGLT-1 cotransports glucose and sodium, which drives passive water uptake. This characteristic has been used for the development of oral rehydration therapy to manage hypersecretory diarrheal disease (24). The potential of SGLT-1-mediated glucose uptake to modulate cell apoptosis has yet to be assessed.

Experimental and clinical data incriminate enteric bacteria in the pathogenesis of acute inflammatory diarrheal disorders and chronic inflammatory bowel diseases (IBD). Bacterial enteritis induced by *E. coli* and *Salmonella enteritica* accounts for a large number of food-borne diarrheal diseases that pose a threat to public health (4, 5). Abnormally high numbers of adherent *Enterobacteriaceae* (e.g., *E. coli*), *Proteobacteria*, and *Bacteroids* have been reported in the ileal mucosa of patients with Crohn's disease (CD) (25, 26). *E. coli* strains isolated from such patients induce cytotoxicity in intestinal epithelial cells in vitro (e.g., Caco-2), which develops apoptosis-like features upon challenge (25). Such increases in bacterial loads in the intestinal mucosa may increase exposure to pathogenic bacterial products, including lipopolysaccharides (LPS), lipoproteins, and proteoglycans. LPS directly induces the production of proinflammatory cytokines, and the activation of NF κ B in intestinal epithelial cells (27, 28). Moreover, up-regulated expression of receptors for LPS, e.g., Toll-like receptor (TLR) -4, has been found in epithelial cells of IBD patients (29), suggesting a potentially increased responsiveness to LPS. The notion that circulating LPS and anti-endotoxin antibodies have been detected in the plasma of IBD patients may imply a breach of the intestinal epithelial barrier (30, 31). Whether apical exposure to high concentration of LPS directly induces epithelial apoptosis and barrier defect in the intestine has yet to be determined.

In the present study, LPS was tested as a stressor model for induction of cell apoptosis. We investigated the caspase-dependent mechanisms of LPS-induced apoptosis, and the rescue pathways used by epithelial cells to correct cell death, focusing on the role of glucose uptake. The aims of this study were to 1)

examine whether apical exposure to high concentration of LPS induce intestinal epithelial cell apoptosis and loss of barrier function, 2) assess whether altered levels of glucose uptake may modulate LPS-induced epithelial defects, 3) determine the role of the specific glucose transporter, i.e., SGLT-1, in the regulation of cell apoptosis and paracellular permeability, and 4) investigate the mechanisms of glucose-mediated cytoprotection.

MATERIALS AND METHODS

Cell culture

SGLT-1-transfected Caco-2 cells (32) were grown in Dulbecco's modified Eagle's medium (DMEM) (Life Technologies, Inc., Gaithersburg, MD, USA) that contained 25 mM of glucose. The media was supplemented with 10% fetal bovine serum (FBS), 15 mM HEPES, 100 U/mL penicillin, and 0.1 mg/mL streptomycin (Sigma, St. Louis, MO, USA), and 0.25 mg/mL Geneticin (Life Technologies) (32). The expression of SGLT-1 protein on the apical membrane of these cells has been previously established (32). Preliminary experiments confirmed the apical, but not basolateral uptake of SGLT-1-dependent radiolabeled sugar from the cell monolayer. Cells were seeded in 96-well tissue culture plates (10^5 cells/well, Costar, Corning, NY, USA), 24-well plates (10^6 cells/well, Costar), 6-well plates (6×10^6 cells/well, Costar), or 12-well transwells, which contained a 1 cm² semipermeable filter membrane with 0.4 μ m pores (10^6 cells/well, Costar). Cells were grown to confluency for 1 wk at 37°C with 5% CO₂ and 96% humidity. In all studies, cells were used between passages 21 and 27.

LPS treatment under low and high glucose media

Confluent cells were exposed to a high concentration (50 μ g/mL) of lipopolysaccharide (LPS, *E. coli* O26:B6, Sigma) in either high glucose (25 mM) or low glucose (5 mM) media for 24 h. The high glucose media was purchased from Life technologies. The low glucose media was made up by 1: 4 ratio of high glucose DMEM and glucose-free DMEM (both from Life Technologies) and supplemented with 20 mM of D-mannitol (Sigma) for osmotic balance. Both media were supplemented with 10% FBS, 15 mM HEPES, 100 U/mL, 0.1 mg/mL penicillin/streptomycin, and 0.25 mg/mL Geneticin.

In some experiments, cells were treated with caspase inhibitors 1 h before addition of LPS under low glucose media to assess the involvement of various caspases in cell apoptosis. Inhibitors to caspase-3 (Z-DEVD-FMK), caspase-8 (Z-IETD-FMK), and caspase-9 (Z-LEHD-FMK) were cell permeable and irreversible (Calbiochem, Biosciences, Inc., La Jolla, CA, USA). All caspase inhibitors were used at a concentration of 120 μ M as described previously (3).

JC-1 assay

The loss of mitochondrial membrane potential is a marker for apoptosis (33). Cells grown in 96-well plates (10^5 cells/well) were treated with LPS for 24 h and incubated with JC-1 reagent for 15 min before fluorescence reading following the manufacturer's instruction. The JC-1 assay kit (Cell Technology Inc., Mountain View, CA, USA) uses a cationic dye (5,5',6,6'-tetrachloro-1,1',3,3'-tetraethylbenzimidazolylcarbocyanine iodide) that aggregates in the mitochondria of

viable cells due to the negative charge established by the electrochemical gradient, and becomes fluorescent red. In apoptotic cells, the dye is dispersed in the cytoplasm due to the loss of mitochondrial membrane potential and remains in the green fluorescent monomeric form.

Cell death detection ELISA

DNA fragmentation, which is the final stage of apoptosis, was measured using a cell death detection ELISA kit as described previously (Roche, Laval, Quebec, Canada) (2, 3). This quantitative sandwich enzyme immunoassay specifically measures the histone region (H1, H2A, H2B, H3, and H4) of mono- and oligonucleosomes that are released during apoptosis. Enterocytes were grown in 24-well plates (10^6 cells/well) until confluency and treated with LPS ($50 \mu\text{g}/\text{mL}$) for 24 h. The proapoptotic topoisomerase-I inhibitor camptothecin ($20 \mu\text{g}/\text{mL}$, Sigma) was used as a positive control for apoptosis after 24 h of incubation. Monolayers were processed according to the manufacturer's instruction. Samples were measured in duplicates. Photometric development was monitored kinetically by reading the plate at 405 nm at 5 min intervals by using a THERMOmax microplate reader (Molecular Devices Corp. Menlo Park, CA, USA). The absorbance units (O.D.) of each group were normalized to total protein amount (mg) (measured by BioRad Dc protein assay, Hercules, CA, USA) since some of the apoptotic cells were found to detach from culture plates. This phenomenon was previously verified by calculating the number of attached cells after the various treatments. Single cells isolated by trypsin-EDTA were counted in blinded fashion using a hemocytometer. Remnant cell numbers for control and LPS-treated samples in low glucose were significantly ($P < 0.05$) different (9.22 ± 0.65 and $5.25 \pm 0.24 \times 10^5$ cells/well, respectively). In contrast, numbers of remnant cells in high glucose levels were not different between both groups (12.81 ± 0.43 and $10.51 \pm 1.18 \times 10^5$ cells/well, respectively; $n = 5/\text{group}$). Cell death values (O.D./mg) were expressed as a ratio of the absorbance of the experimental cell lysates to that of controls (arbitrarily set at 100%) after 10 min of development. The detection limit for this ELISA is 10^2 apoptotic cells.

Paracellular permeability studies

Cells were grown in transwells (10^6 cells/well, 1 cm^2 surface area of filter membrane) until confluency, and exposed to apical LPS under low or high glucose media for 24 h. TER was measured using an electrovoltmeter (EVOM; World Precision Instruments, Sarasota, FL, USA). The transfected Caco-2 cell line used in this study developed electrical resistances of $\sim 271.0 \pm 4.4 \text{ Ohms}/\text{cm}^2$ upon confluency. Paracellular permeability was assessed by apical-to-basal transport of a Dextran probe (MW3000) conjugated to fluorescein (Molecular Probes, Eugene, OR, USA) as described previously (2, 3). Briefly, monolayers were washed gently two times with sterile bicarbonate-buffered Ringer's solution (37°C). Dextran-fluorescein at $100 \mu\text{M}$ in Ringer's solution was added into the apical chamber and Ringer's solution was added to the basolateral compartment. After 3 h of incubation (37°C in 5% CO_2 , 96% humidity), two $300 \mu\text{L}$ samples were collected from the basal chamber for fluorometric measurement on a microplate fluorometer (SpectraMax Gemini, Molecular Devices, Sunnyvale, CA, USA) with an excitation wavelength of 496 nm, emission at 524 nm, and cutoff at 515 nm. Paracellular permeability to dextran was expressed as percentage of apical flux per cm^2/h . In some experiments, inhibitors of myosin light chain kinase (ML-9, $40 \mu\text{M}$) (34) or Rho kinase (Y27632, $50 \mu\text{M}$) (35) (Sigma) were added prior to LPS challenge in

low glucose media to examine the involvement of these kinases in LPS-induced barrier defects.

Sugar uptake assay

Cells grown on transwells (10^6 cells/well) were exposed to apical LPS in cell culture media with low or high glucose for 24 h as described above. Sugar uptake was measured with a radioassay using a nonmetabolized C^{14} -labeled sugar probe, α -methyl glucopyranoside (α -MG) (Amersham Biosciences, Quebec, Canada). The α -MG sugar probe selectively binds to SGLT-1, and is not transported by other glucose transporters (23, 32). Briefly, cells were gently washed with glucose-free Hank's balanced salt solution supplemented with 25 mM D-mannitol (mannitol-HBSS) and then incubated apically with 0.2 mL of mannitol-HBSS containing $2 \mu\text{Ci}/\text{mL}$ ^{14}C -labeled for 30 min at 37°C , 5% CO_2 , and 96% humidity. Cells were washed with HBSS at 4°C , solubilized with 0.1 N NaOH, and the lysate was then mixed into Ready safe liquid scintillation cocktail (Beckman Coulter, Fullerton, CA, USA). The level of sugar uptake was measured using a β -scintillation counter, and values expressed as moles of α -MG/ cm^2 . Selective uptake of the α -MG sugar probe by SGLT-1 was verified by a blockage study using 0.5 mM phloridzin (Sigma). Phloridzin is a glucose analog that specifically inhibits SGLT-1, but is not transported into cells and does not affect intracellular glucose metabolism. Phloridzin has a higher affinity compared with α -MG or D-glucose for binding to SGLT-1 (23, 32). Previous studies have demonstrated that α -MG uptake is linear from 15 min to at least 2 h (32). The level of SGLT-1-mediated sugar uptake in each treatment group was presented as the percentage of that measured in control cells in low glucose media.

Extraction of whole cell lysate

Cells grown in 6-well plates (6×10^6 cells) and exposed to LPS for 24 h were processed for Western blot. Briefly, cells were lysed with RIPA buffer (1% Nonidet P-40, 0.5% sodium deoxycholate, 0.1% SDS, and one tablet of complete-Mini[®] protease inhibitors cocktail (Roche, Penzberg, Germany) added to 10 mL of buffer immediately before use). The lysates were centrifuged at 14000 g for 10 min and supernatant was collected. Protein assay (BioRad Dc protein assay) was performed, and concentrations adjusted to 5 mg/mL. The supernatant was dissolved in $2 \times$ electrophoresis sample buffer containing 2% (w/v) SDS, 100 mM DTT, and 62.5 mM Tris/HCl (pH 6.8) at a 1:1 ratio, and subjected to 95°C heat block for 5 min for denaturation. Samples were frozen at -20°C until use for immunoblotting of caspase-3, Bcl-2, Bcl-X_L and Bax (see below).

Extraction of cytosolic and membrane-bound fractions

Cytosolic and membrane-bound extracts were prepared by selective permeabilization with digitonin and Triton X-100, respectively, as described previously (36). Cells were grown in 6-well plates to confluency and exposed to LPS under low and high glucose. Cell monolayers were washed with PBS twice, and incubated with 0.05% digitonin in isotonic buffer for 3 min at room temperature. Isotonic buffer contained 250 mM sucrose, 10 mM HEPES, 10 mM KCl, 1.5 mM MgCl₂, 1 mM EDTA, 1 mM EGTA, pH 7.1. Complete-Mini[®] protease inhibitor cocktail (Roche) was added to the isotonic buffer immediately before extraction. The supernatant was collected without agitating the attached monolayer and centrifuged at 14000 g for 10 min to dispose of suspending cells. The resultant proteins in the digitonin-soluble fractions (cytosolic

fraction) were concentrated to 3 mg/mL with 10K cutoff microcon® centrifugal filter device (Millipore, Billerica, MA, USA). Cytosolic fractions were dissolved in electrophoresis sample buffer. The samples were frozen at -20°C until use for immunoblotting of cytochrome *c*.

The remained attached monolayers were subsequently lysed with 1% (v/v) Triton X-100 in isotonic buffer for 10 min at 4°C. The lysate was collected and centrifuged at 14000 *g* for 10 min. The resultant supernatant was collected, and the protein concentration in this Triton X-soluble fraction (membrane-bound fraction) was adjusted to 2 mg/mL and dissolved in electrophoresis sample buffer. Samples were frozen at -20°C until use for immunoblotting of VDAC and cytochrome *c*.

Western blot for caspase-3, occludin, Bcl-2, Bcl-X_L, Bax, VDAC, and cytochrome *c*

Proteins in cytosolic and membrane-bound fractions, and whole cell lysates were subjected to reducing SDS/PAGE (4–13% polyacrylamide). The resolved proteins were then electroblotted onto Hybond-P PVDF membranes (Amersham Biosciences, Piscataway, NJ, USA). After 1 h blocking at room temperature in 5% nonfat dry milk, the membranes were incubated with primary antibody overnight. Membranes were washed three times with Tris-buffered saline (TBS) with 0.1% Tween 20 for 5 min and incubated with secondary horseradish peroxidase-conjugated antibodies at room temperature for 1 h. Antigens on the membranes were then revealed by exposure to chemiluminescent substrates (ECL plus Western blot detection system, Amersham Biosciences, Buckinghamshire, England). Precision Plus protein™ standards (Bio-Rad, Hercules, CA, USA) were used as molecular weight markers for protein electrophoresis. Band density was measured by photoimage analysis using the Quantity one software (Bio-Rad).

Caspase-3 cleavage is a hallmark of the apoptosis effector pathways. A polyclonal rabbit anti-human caspase-3 antibody (Cell Signaling Technology Inc., Beverly, MA, USA), which recognized both the full-length and cleaved form of caspase-3 were used for immunoblotting of whole cell lysates. Changes in the tight junctional occludin level were assessed using a monoclonal mouse anti-human occludin antibody (Zymed, San Francisco, CA, USA). Primary antibodies used for the detection of Bcl-2, Bcl-X_L, and Bax in whole cell lysates included polyclonal rabbit anti-human Bcl-2 antibody (Oncogene, San Diego, CA, USA), monoclonal mouse anti-human Bcl-X_L antibody (Calbiochem, La Jolla, CA, USA), and polyclonal rabbit anti-human Bax antibody (Oncogene). Rabbit polyclonal anti-VDAC antibody (Santa Cruz Biotechnology, Santa Cruz, CA, USA) or mouse monoclonal anti-cytochrome *c* antibody (R&D systems, Cedarlane Lab.) was used as the primary antibodies for immunoblotting in cytosolic and membrane-bound fractions. Primary antibody to actin (mouse monoclonal anti-human actin, Mediacorp, Montreal, QC) was used to control for equal loading in each sample. Secondary goat anti-rabbit IgG and goat anti-mouse IgG conjugated with horseradish peroxidase were purchased from Santa Cruz Biotechnology.

Statistical analysis

All values were expressed as mean ± standard error. Statistical significance was determined by one-way ANOVA (ANOVA) followed by Tukey's compromise test for multiple comparisons, or paired Student's *t* test, where appropriate. Significance was established at *P* < 0.05.

RESULTS

1. LPS induces caspase-8-, -9-, and -3-dependent apoptosis in intestinal epithelial cells

SGLT-1-transfected Caco-2 cells were exposed to apical LPS isolated from *E. coli* O26:B6 in low glucose (5 mM) media and assessed for apoptosis. Levels of apoptosis in control cells at either low glucose or high glucose were not different (Original O.D. values were 1.023±0.037 and 1.157±0.068, respectively [*n*=6/group]). Preliminary data demonstrated that LPS-induced apoptosis was dose-dependent (data not shown). Exposure to LPS (50 µg/mL) in low glucose media induced a significant reduction (~31%) of mitochondrial membrane potential in intestinal epithelial cells (Fig. 1A). Accumulation of JC-1 dye in the aggregated form (red fluorescence) was observed in the mitochondria of control cells in low glucose media (Fig. 2A). In contrast, after exposure to LPS in low glucose, monomeric dye dispersed in the cytoplasm and displayed green fluorescence, indicating the collapse of mitochondrial membrane integrity (Fig. 2B). To identify downstream effectors in the apoptotic signaling pathway, caspase-3 cleavage was examined by Western blot. LPS treatment in low glucose media resulted in cleavage of caspase 3 (~35 kDa) into two distinct smaller molecular weight fragments (~17 kDa and ~19 kDa) (Fig. 1B). Apoptosis was further assessed by measuring the formation of oligonucleosomes. In low glucose media, LPS significantly increased cell apoptosis (Fig. 1C). To further characterize the pathways of LPS-induced apoptosis, caspase inhibitors were added prior to LPS treatment in low glucose, and DNA fragmentation measured. Inhibition of the common downstream effector, caspase-3, prevented LPS-induced cell apoptosis. Addition of either caspase-8 or -9 inhibitors also blocked LPS-induced cell apoptosis (Fig. 1D).

2. LPS stimulation results in reduction of TER and increased paracellular permeability in intestinal epithelial cells

Previous studies have suggested that heightened enterocyte apoptosis may disrupt epithelial barrier function (3, 10). Results from the present experiments demonstrated that exposure to LPS in low glucose conditions significantly reduces TER in epithelial monolayers (Fig. 3A, B). Addition of caspase-3 inhibitor abolished the barrier defect induced by LPS in low glucose (Fig. 3A). Consistent with the barrier defect, exposure to LPS in low glucose media also significantly increased the apical-to-basal translocation of dextran in monolayers (Fig. 3C).

Epithelial cell apoptosis may lead to elevation of paracellular permeability, either from circumferential contraction via perijunctional actomyosin ring, or through disruption of tight junctional structures (2, 3, 34). Phosphorylation of the light chain of myosin II band by myosin light chain kinase (MLCK) (37) or Rho kinase (38, 39) causes contraction of the myosin band.

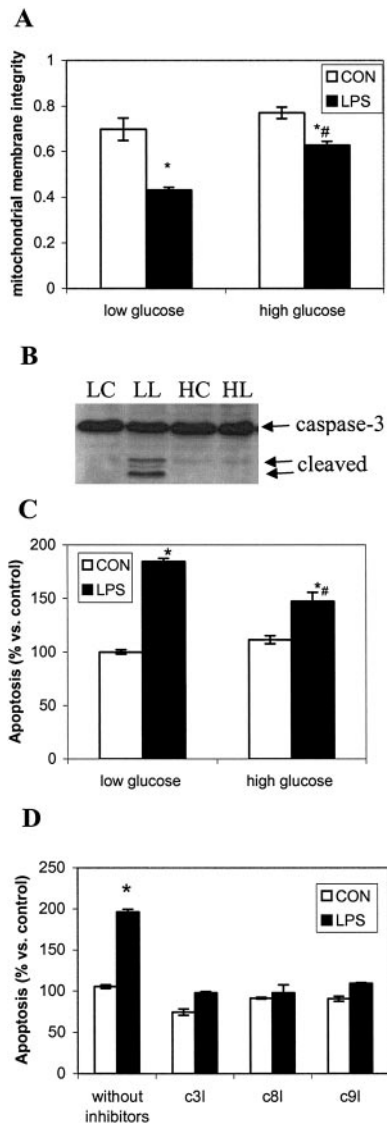


Figure 1. LPS induces caspase-8-, -9-, and -3-dependent apoptosis in intestinal epithelial cells in low glucose conditions. Presence of high glucose rescues intestinal epithelial cells from LPS-induced apoptosis. *A*) Caco-2 cells were untreated (open bars) or exposed to LPS (filled bars), and loss of mitochondrial membrane potential (an early event of apoptosis) was measured. Mitochondrial membrane integrity was expressed as ratios of red vs. green fluorescence units. $n = 4/\text{group}$. $*P < 0.05$ compared with respective controls. $\#P < 0.05$ compared with LPS-treated cells under low glucose group. *B*) Representative Western blot image from 3 independent experiments illustrating caspase-3 cleavage upon exposure to LPS in low (LL) but not high glucose (HL) compared with their respective sham-treated controls (LC, HC). *C*) untreated (open bars) and LPS-treated cells (filled bars) were assessed for the formation of apoptotic oligonucleosomes. Levels of cell apoptosis were normalized to the total amount of protein, and illustrated as percentage vs. control values in low glucose. $*P < 0.05$ compared with respective controls. $\#P < 0.05$ compared with LPS-treated cells in low glucose. $n = 6/\text{group}$. *D*) Inhibitors of caspase-3 (c3I), caspase-8 (c8I), or caspase -9 (c9I) block LPS-induced cell apoptosis in low glucose conditions. Cells were either untreated (open bars) or LPS-treated (filled bars), in the presence or absence of caspase inhibitors. $n = 3/\text{group}$. $*P < 0.05$ compared with respective controls.

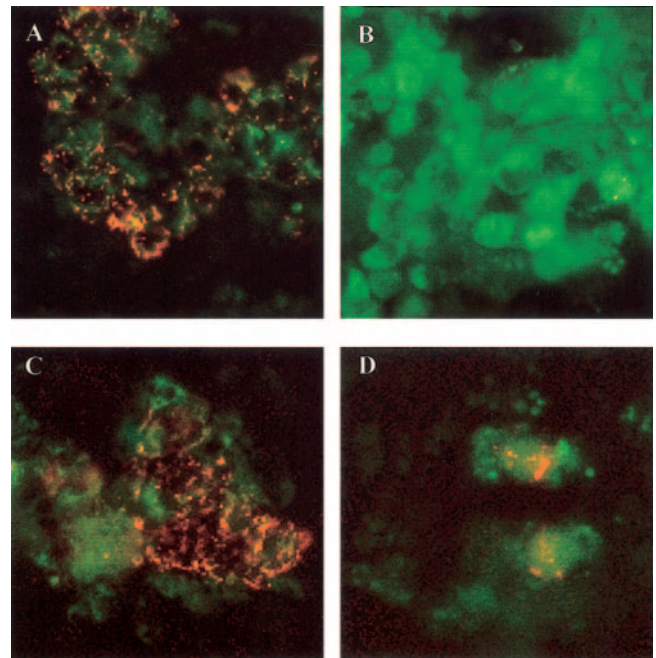


Figure 2. Representative images of mitochondrial integrity in control and LPS-treated cells in low and high glucose media. The aggregated form of JC-1, characteristic of mitochondrial integrity (red fluorescence), was observed in control cells in low glucose (*A*) and high glucose (*C*). Exposure to LPS in low glucose eliminated JC-1 aggregates (red fluorescence) and induced significant dispersion of monomeric JC-1 (green fluorescence) throughout the cytoplasm (*B*), suggesting a loss of mitochondrial membrane potential. Presence of high glucose maintained at least in part the presence of JC-1 aggregates (red fluorescence), and prevented the release of the monomeric JC-1 (green fluorescence) into the cytoplasm after LPS (*D*). Results from fluorometric analysis are presented in Fig. 1A. All micrographs were obtained at an original magnification of 400 \times .

Contraction of myosin in turn acts on the attached F-actin that is linked to tight junctional proteins resulting in increased paracellular permeability. Inhibitors of MLCK (ML-9) and Rho kinase (Y27632) were used to investigate the involvement of myosin light chain in barrier defect induced by LPS. The addition of ML-9 and Y27632 did not affect the LPS-induced increased paracellular permeability in low glucose media (**Fig. 4A**). To assess changes in the tight junctional structure after apoptosis, the level of transmembrane protein occludin was investigated by Western blot. Cleavage of occludin was observed after exposure to LPS in low glucose media (**Fig. 4B**).

3. High glucose rescues epithelial cells from LPS-induced apoptosis and barrier defects

Apoptosis is an energy-dependent process. Mitochondrial oxidative phosphorylation of glucose derivatives accounts for energy production in the cells. The involvement of mitochondrial pathways in the LPS-induced apoptosis prompted the investigation of the role of glucose in modifying the level of cell death. In high

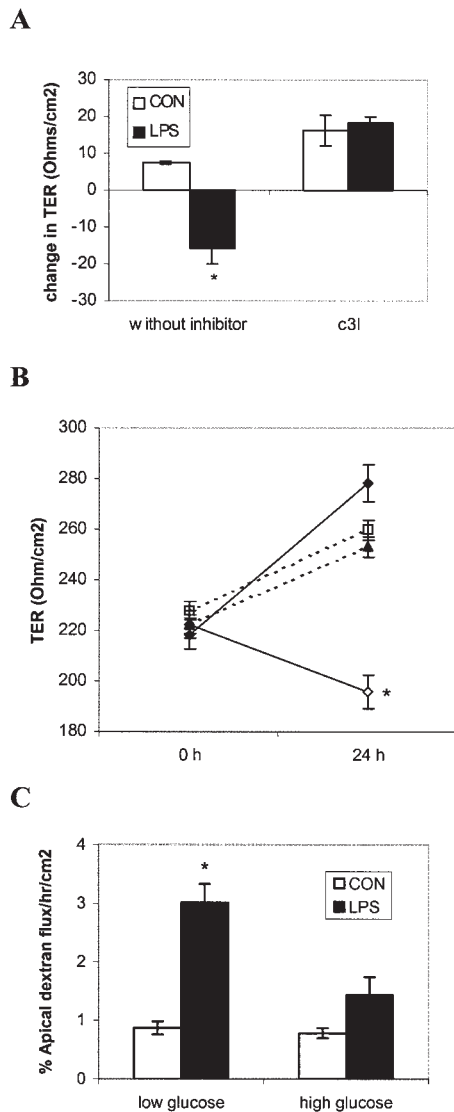


Figure 3. LPS disrupts barrier function in intestinal epithelial monolayers. *A*) LPS-induced reduction of the transepithelial resistance (TER) in low glucose media was abolished in the presence of caspase-3 inhibitor. Values are expressed as changes in TER from time 0 to 24 h. $n = 3/\text{group}$. $*P < 0.05$ compared with respective control groups. *B*) TER of cell monolayers that were either untreated (◆) or LPS-treated (—◇—) under low glucose media; or, untreated (-▲-) or LPS-treated (-◆-) under high glucose conditions. $n = 6/\text{group}$. $*P < 0.05$ compared with respective control groups. *C*) Exposure to apical LPS in low glucose, but not high glucose, significantly increases apical-to-basolateral translocation of dextran-fluorescein across epithelial monolayers. $n = 3/\text{group}$. $*P < 0.05$ vs. respective controls.

glucose (25 mM) conditions, the loss of mitochondrial membrane integrity caused by LPS was significantly attenuated when compared with values obtained under low glucose (Fig. 1A). Images illustrating the presence of intact mitochondria that displayed aggregated JC-1 (red fluorescence) in control cells under high glucose media are shown in Fig. 2C. Cells that were exposed to LPS in high glucose maintained the aggregated JC-1 (Fig. 2D), though at lower levels than in control (Fig. 2C). Cytoplasmic appearance of monomeric JC-1

(green fluorescence) seen in the LPS-treatment group in high glucose (Fig. 2D) was less prevalent than that detected in low glucose media (Fig. 2B). LPS-induced cleavage of caspase-3 detected in low glucose media was abolished when cells were grown in high glucose conditions (Fig. 1B). In high glucose media, cells treated with LPS also displayed significantly lower levels of DNA fragmentation than those grown under low glucose conditions (Fig. 1C). Baseline levels of cell apoptosis under high glucose media (258.6 ± 5.5 O.D./mg) were not significantly different from those in low glucose media (212.7 ± 7.2 O.D./mg), indicating that high glucose does not alter baseline, i.e., physiological, apoptosis. Cells in suspension accounted for $< 10\%$ of the total number of apoptotic cells and the levels were not significantly different among groups (data not shown).

TER or transepithelial fluxes of FITC-dextran were measured in separate sets of experiments to assess epithelial permeability. LPS-induced reduction of TER and increased paracellular permeability in low glucose was completely abolished in the presence of high glucose (Fig. 3B, C). The amount of apical-to-basal

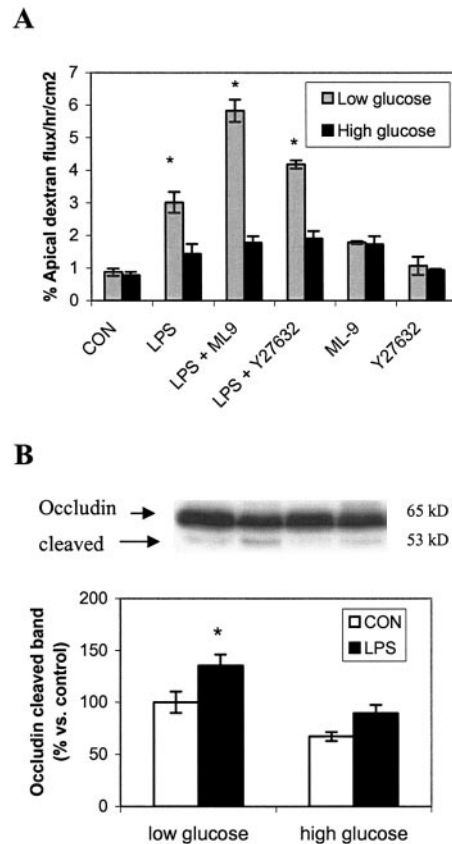


Figure 4. LPS-induced barrier defects involve the degradation of tight junctional occludin protein. *A*) Addition of inhibitors of myosin light chain kinase (ML-9) and Rho kinase (Y27632) did not inhibit LPS-induced increased paracellular permeability to dextran in low glucose media. $*P < 0.05$ compared with respective controls. *B*) LPS-induced cleavage of occludin in low glucose media is inhibited by the presence of high glucose. Western blots from 3 independent experiments were quantified by densitometry. $*P < 0.05$ compared with respective controls.

translocation of dextran-fluorescein was minimal (~3% of total fluorescence) in both untreated and LPS-treated cells in the presence of high glucose media, indicating the maintenance of intact barrier function by these monolayers (Fig. 3C). Baseline TER and dextran permeability of control cells under low and high glucose media were not significantly different. Presence of high glucose also inhibited the cleavage of occludin induced by LPS (Fig. 4B).

4. LPS up-regulates SGLT-1-mediated sugar uptake under high glucose media

Results indicate that increased glucose availability may modulate cytoprotection from LPS-induced apoptosis. To further investigate the role of glucose transport in this mechanism, another set of studies assessed uptake of a radiolabeled SGLT-1-specific sugar, α -MG. The level of sugar uptake was not different between control cells in low and high glucose media (Fig. 5A). In high glucose media, cells exposed to LPS showed a twofold increase in sugar uptake compared with that of controls (Fig. 5A). In contrast, in low glucose media, sugar uptake was not different between LPS-exposed and control cells (Fig. 5A). Moreover, sugar uptake in both baseline and LPS-challenge conditions (not shown) could be inhibited by adding phloridzin in the radioactive α -MG solution.

5. Blockage of SGLT-1 sugar uptake inhibits the anti-apoptotic effect of high glucose media

Other experiments then investigated whether blockage of SGLT-1 activity by phloridzin during LPS treatment may inhibit the cytoprotective effects observed in high glucose media. Addition of phloridzin during exposure to LPS in high glucose media inhibited SGLT-1-mediated sugar uptake in a dose-dependent manner (Fig. 5B). Phloridzin at 2 mM was chosen as the dosage to inhibit ~65% of control sugar uptake to conduct subsequent studies. Previous studies have established that 2 mM of phloridzin is sufficient to inhibit SGLT-1-mediated transport in 3–5 mM glucose (37, 40). As illustrated in Fig. 5C, LPS-induced apoptosis was significantly attenuated vs. values obtained in low glucose, consistent with the previous experiments. This inhibitory effect was abolished with the addition of phloridzin, as cell apoptosis was increased to levels ($180 \pm 0.3\%$) similar to those measured in LPS-challenged cells in low glucose without phloridzin ($185 \pm 2.8\%$) (Fig. 5C). Phloridzin alone did not alter the level of epithelial cell apoptosis (Fig. 5C).

6. Inhibition of SGLT-1 activity blocks the glucose-mediated rescue from barrier defects caused by LPS

In monolayers treated with LPS in high glucose, inhibition of glucose uptake by phloridzin reduced TER values to levels comparable to those of LPS-treated cells in low glucose media. Phloridzin treatment under low

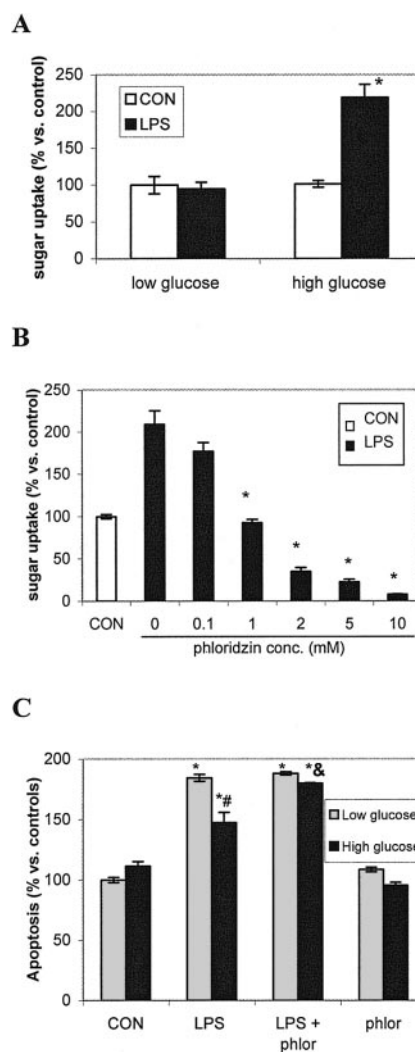


Figure 5. Blockage of SGLT-1-mediated sugar uptake by phloridzin prevents the cytoprotection exerted by high glucose. *A*) SGLT-1-mediated sugar uptake after LPS challenge increased in intestinal epithelial cells under high, but not low, glucose conditions. Sugar uptake was expressed as a percentage of values measured in control cells in low glucose media. * $P < 0.05$ compared with respective controls. $n = 6$ /group. *B*) phloridzin inhibition of LPS-induced increased SGLT-1-mediated sugar uptake under high glucose media is dose-dependent. $n = 3$ /group. *C*) addition of phloridzin during exposure to LPS increases the level of apoptosis (DNA fragmentation) compared with LPS treatment alone in high glucose media. Phloridzin alone does not change the level of apoptosis in both low and high glucose conditions. Levels of cell death were normalized to total protein. * $P < 0.05$ compared with respective untreated controls. # $P < 0.05$ compared with cells exposed to LPS in low glucose. and $P < 0.05$ compared with cells exposed to LPS in high glucose. $n = 6$ /group.

glucose media further reduced TER in LPS-treated preparations (Fig. 6A).

To confirm the role of SGLT-1-mediated sugar uptake in the maintenance of barrier function upon LPS challenge, another set of studies investigated the effects of phloridzin on dextran fluxes. Inhibition of SGLT-1-mediated glucose uptake by phloridzin increased the

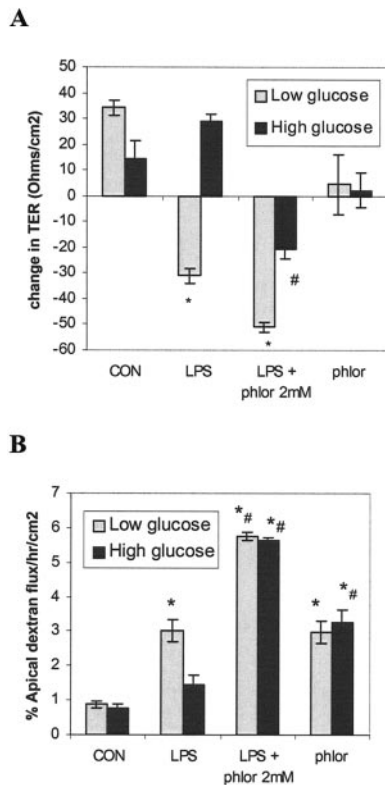


Figure 6. Blockage of SGLT-1 activity by phloridzin inhibits glucose-mediated protection against LPS-induced changes in paracellular permeability. *A*) Change of TER in low (gray bar) and high (black bar) glucose conditions after 24 h treatment with sham controls (CON), LPS, LPS plus 2 mM phloridzin (LPS + phlor), or phloridzin alone (phlor). Values are expressed as changes in TER from time 2 to 24 h. $n = 3/\text{group}$. * $P < 0.05$ compared with respective controls. # $P < 0.05$ compared with respective LPS treatment groups. *B*) Paracellular permeability to dextran-fluorescein after LPS treatment under low (gray bar) and high (black bar) glucose conditions for the same experimental groups as in *A*. $n = 3/\text{group}$. * $P < 0.05$ compared with respective controls. # $P < 0.05$ compared with respective LPS treatment groups.

translocation of dextran-fluorescein in monolayers treated with LPS under both low and high glucose media (Fig. 6*B*).

7. Mechanisms of glucose-mediated cytoprotection: role of Bcl-2, Bcl-X_L, and Bax

In an attempt to gain a better understanding of how sugar uptake may modulate apoptosis, the expression of anti-apoptotic proteins, Bcl-2 and Bcl-X_L, and the proapoptotic protein, Bax, was measured by Western blot and densitometric analysis. In low glucose media, levels of Bcl-2 significantly decreased (~60%) in cells exposed to LPS compared with controls (Fig. 7*A*). This decrease was inhibited in the presence of high glucose, and Bcl-2 levels were no longer different between LPS-treated and control groups (Fig. 7*A*). Moreover, analysis of Bcl-X_L demonstrated no statistical difference between LPS-treated and control groups under low glucose media. In contrast, in the presence of high

glucose, increased amounts (235 ± 37.5% vs. control) of Bcl-X_L were detected after LPS treatment (Fig. 7*B*). The total amount of Bax did not change after LPS treatment either under high or low glucose media (Fig. 7*C*).

Additional experiments measured Bcl-2 with ELISA. The results confirmed that total Bcl-2 levels were significantly reduced in LPS-treated cells under low glucose condition. In contrast, in the presence of high glucose, levels of total Bcl-2 remained unchanged after exposure to LPS (Fig. 8*A*). Amount of the active, phosphorylated form of Bcl-2 was also measured. LPS treatment under low glucose media decreased the level of the phospho-

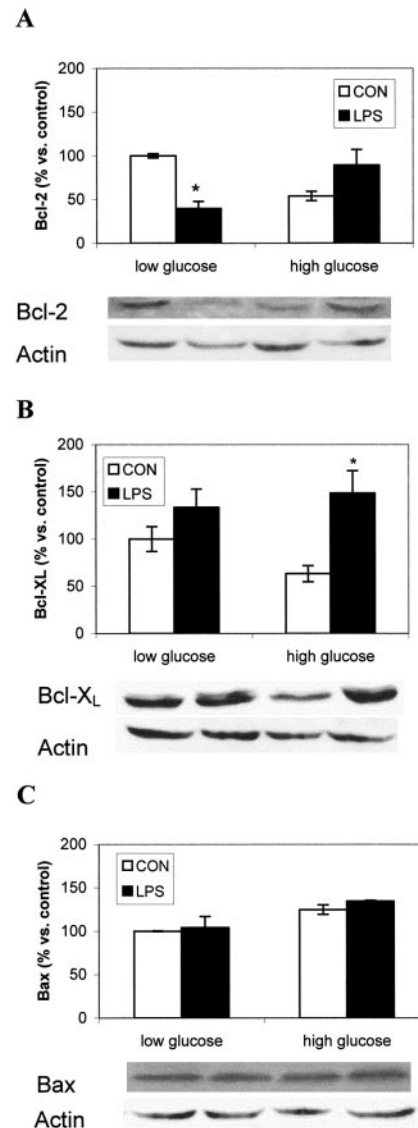


Figure 7. Representative Western blot images and densitometric analyses of Bcl-2, Bcl-X_L, and Bax in control and LPS-treated monolayers. Cells were untreated or treated with LPS under low glucose media (LC and LL, respectively), or under high glucose media (HC and HL, respectively). The figures illustrate data for Bcl-2 (*A*), Bcl-X_L (*B*), and Bax (*C*). Images are representative of 3 separate experiments. Band density was measured and expressed as the percentage of their respective untreated controls. $n = 3/\text{group}$. * $P < 0.05$ compared with respective controls.

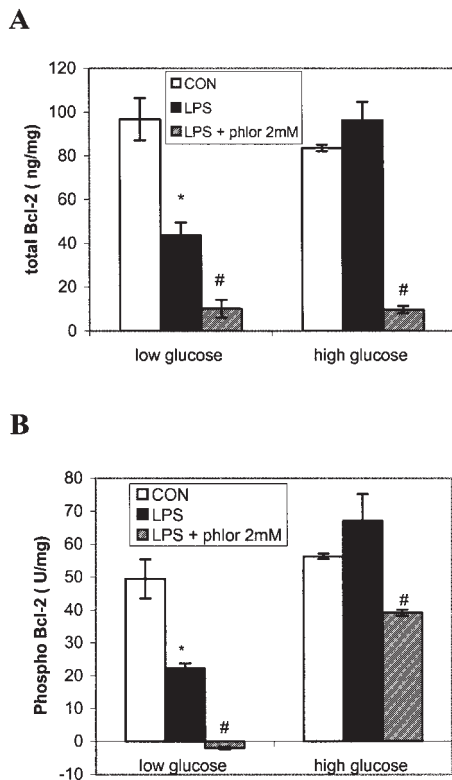


Figure 8. High glucose prevents the LPS-induced reduction of total and phosphorylated Bcl-2 levels in epithelial cells. The amounts of total Bcl-2 (A) or phosphorylated Bcl-2 (Panel B) in control (CON) and LPS-treated cells (LPS), or cells exposed to LPS in the presence of 2 mM phloridzin (LPS+phlor), under low and high glucose media. $n = 9$ /group. * $P < 0.05$ compared with respective controls. # $P < 0.05$ compared with LPS treatment group.

ylated form of Bcl-2. In contrast, LPS-induced reduction of Bcl-2 phosphorylation was abolished in the presence of high glucose (Fig. 8B).

Addition of phloridzin during LPS challenge significantly reduced the level of total Bcl-2 compared with the LPS groups in both low and high glucose media (Fig. 8A). Phloridzin also decreased the levels of phosphorylated Bcl-2 (Fig. 8B).

8. High glucose inhibits translocation of cytochrome *c* from mitochondria to cytosol after LPS treatment

Cytochrome *c* release was measured in membrane-bound and cytosolic fractions of cells after digitonin and Triton X-100 permeabilization. In the absence of LPS, in cells under low or high glucose media, cytochrome *c* was exclusively mitochondrial, i.e., in the membrane fraction. In contrast, after LPS treatment in low glucose media, the presence of cytochrome *c* was detected in the cytosolic fractions. High glucose conditions inhibited the release of cytochrome *c* into the cytosol (Fig. 9A).

Epithelial cell membrane fraction (containing mitochondrial proteins) and cytosolic fractions were assessed for levels of VDAC (a mitochondrial outer

membrane protein) to control for membrane contamination in the cytosolic fraction (Fig. 9B). Immunoblotting results showed that VDAC was not detectable in any of the digitonin-soluble (cytosolic) fractions of any of the four groups. The level of VDAC in Triton membrane-bound fraction increased after LPS treatment in both low and high glucose conditions (Fig. 9B).

DISCUSSION

Excessive epithelial cell apoptosis induced by enteric pathogens compromises intestinal barrier function. These abnormalities have been implicated in the pathogenesis of IBD, protozoal infection, and bacterial enteritis. Consistent with these observations, the present findings demonstrate that bacterial LPS, used as a microbial stressor model, may directly induce cell apoptosis and increase epithelial paracellular permeability. In view of the broad biological implications of these phenomena, this study explored mechanisms of cellular rescue from LPS-induced apoptosis. The results identify a novel pathway through which SGLT-1-mediated glucose uptake protects the intestinal epithelium against LPS-induced apoptosis and barrier defects by

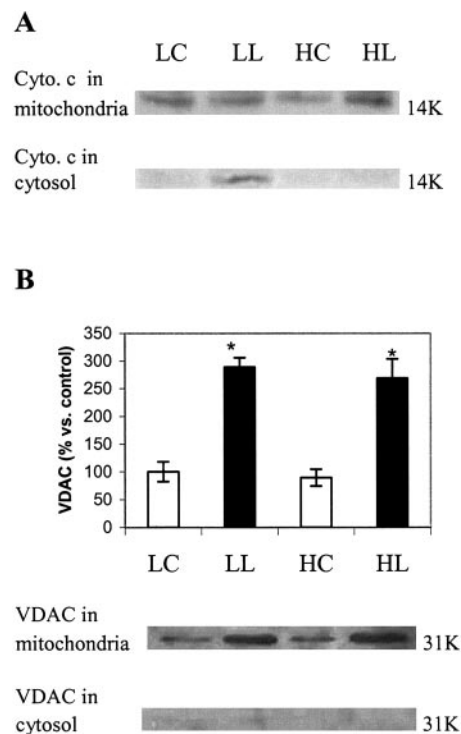


Figure 9. Effects of high glucose on VDAC expression and translocation of mitochondrial cytochrome *c* to the cytosol after exposure to LPS. Cells were untreated (LC) or exposed to LPS (LL) under low glucose media, or under high glucose media (HC and HL, respectively). The figure illustrates results from immunoblotting of cytochrome *c* (A) or VDAC (B) in membrane-bound or cytosolic cell fractions. Images shown are representative blots from 3 independent experiments. * $P < 0.05$ compared with respective controls.

preserving anti-apoptotic Bcl-2 activity and enhancing Bcl-X_L.

In a number of intestinal disorders, including infection with pathogenic Gram-negative bacteria and IBD, the small intestinal mucosa is abnormally exposed to high concentrations of microbial products, e.g., LPS. These observations offer a rationale for the high doses of apical LPS tested in the present study. In normal rats, the mean LPS concentration detected in luminal contents of the terminal ileum is ~1.8 µg/mL (41). Using the jejunum and ileum of rats, rabbits, and monkeys, as well as Caco-2 cell lines, previous studies on the effects of pathological doses of LPS on epithelial homeostasis and bacterial translocation have used 50–200 µg/mL of apical LPS (42–45). The LPS concentrations required to induce pathology from the apical side of the epithelium are higher than those needed to induce systemic disease, which vary from 200 ng/mL to 10 µg/mL. Bacterial LPS is known to induce a number of cytopathological effects in the intestine. Endotoxemia in mice enhances mucosal permeability to luminal probes, and increases bacterial translocation to the mesenteric lymph node, liver and spleen (46). Elevated production of proinflammatory cytokines, reactive oxygen species, and nitric oxide synthases has been reported in intestinal epithelial cell lines exposed to LPS, and in the endotoxemic mouse intestine (46, 47). In addition, LPS causes vacuolar degeneration and cell death in vascular endothelium, hepatocytes, respiratory and renal epithelial cells (48–51), modulates the expression of adhesion molecules and receptors for growth factors and kinins on endothelial cells (52–54), and stimulates bone absorption by induction of osteoclast formation (55). Whether high doses of luminal LPS may lead to intestinal epithelial cell death and/or disruption of epithelial barrier remains unknown.

The findings reported here demonstrate that apical exposure to high concentrations of *E. coli* LPS directly induces epithelial cell apoptosis in low glucose environments, as evidenced by a loss of mitochondrial membrane potential, cleavage of caspase 3, and fragmentation of DNA. Additional experiments using selective caspase inhibitors prior to LPS challenge showed that LPS-induced apoptosis is dependent on caspase-8, -9, and -3. Together, the findings imply that LPS may induce apoptosis via caspase-8 and the caspase-9-dependent mitochondrial pathway. The receptors involved have yet to be identified. The correlation of epithelial cell apoptosis and disruption of barrier function remains controversial. Our previous studies as well as others have demonstrated that enhanced enterocytic apoptosis may result in increased epithelial permeability, which can be abrogated by pretreatment with caspase inhibitors (3, 9, 10). Conversely, extrusion of apoptotic renal epithelial cells induced by UV light by their neighbors via an actin- and myosin-dependent mechanism has been documented. During this process, the barrier function was maintained (56), similar to the events observed during physiological extrusion of apoptotic enterocytes (1). In the present study, LPS

exposure in low glucose environments reduced trans-epithelial resistance (TER), and increased epithelial paracellular permeability to dextran MW3000. The LPS-induced disruption of barrier function in low glucose environment is dependent on caspase-3, suggesting that epithelial apoptosis may lead to increased paracellular permeability.

Enhanced epithelial paracellular permeability may result from disruptions of tight junctional proteins or contraction of the perijunctional actinomyosin ring (PAMR). Myosin light chain (MLC) -dependent contraction of the PAMR has been observed in pathological events, including infection with *Giardia duodenalis*, and activation of apical protease-activated receptors on the enterocyte membrane (2, 34). A recent study demonstrated that disruption of mitochondrial metabolism by a chemical stressor alters the barrier functions of the intestinal epithelium, and induces increased epithelial permeability and translocation of commensal *E. coli* (57). The results shown here indicate that LPS exposure, in a low glucose environment, induces the cleavage of tight junctional occludin, which is associated with increased paracellular permeability. Moreover, inhibition of MLCK or Rho kinase did not affect the LPS-induced barrier defects. Recent studies have identified caspases and metalloproteases as the enzymes that cleave full-length occludin into smaller fragments in cases of apoptosis (58). Studies in endotoxemic mice have also demonstrated that intravenous injection of LPS induces decreased expression of Zonula occludens (ZO) -1, -2, -3, and occludin in the ileal and colonic mucosa (59). Taken together, these observations suggest that LPS exposure in low glucose conditions may degrade tight junctional occludin leading to elevated paracellular permeability.

The involvement of the mitochondrial pathway in LPS-induced apoptosis suggests a disruption of energy production that mainly relies on mitochondrial oxidative phosphorylation of glucose derivatives. This prompted us to investigate the possibility that glucose uptake may modify the levels of LPS-activated apoptosis. The baseline parameters of epithelial cells in high vs. low glucose media were first examined. The presence of high glucose per se did not alter baseline apoptosis. TER in epithelial monolayers in high vs. low glucose conditions was not statistically different. There was no difference in the permeability to dextran (MW3000) between the two groups. Moreover, the SGLT-1 activities were comparable in epithelial cells between high and low glucose conditions. Previous studies showed that activation of SGLT-1 by glucose supplementation reduces transepithelial resistance, and increases paracellular permeability to small solutes (i.e., mannitol MW 180), but not large molecules (i.e., inulin MW 5000), in human intestines in vivo as well as in epithelial cell lines (37, 40). This glucose-activated, MLC-dependent elevation of paracellular permeability may represent a physiological mechanism for increased sugar absorption during a meal (37). In the present study, we describe a novel role for SGLT-1 that corrects

heightened epithelial apoptosis and tight junctional disruption.

In contrast to the observation made in low glucose media, levels of apoptosis induced by LPS were significantly attenuated in the presence of high glucose. Both LPS-induced barrier defects, i.e., reduction of TER and increased paracellular permeability to dextran, were completely abolished in high glucose media. High glucose also prevented the degradation of tight junctional occludin that corresponds with the maintenance of barrier function. The role of SGLT-1 in this glucose-mediated cytoprotective mechanism was further assessed. LPS challenge significantly increased SGLT-1-mediated sugar uptake in intestinal epithelial cells in high glucose media, but not in low glucose environments. This represents the first observation documenting that microbial factors may stimulate host cells to increase active sugar uptake. Addition of 2 mM phloridzin during LPS exposure inhibited ~60% of the total SGLT-1-specific sugar uptake, and reversed the cytoprotection mediated by high glucose. The involvement of other glucose transporters, such as the basolateral GLUT-2, can be ruled out since the presence of phloridzin completely abolished the glucose-mediated cytoprotection. In addition, the glucose concentrations in the high glucose media exerted cytoprotection at 25 mM, which is below the known levels required for saturation (30–50 mM) and induction of GLUT-2 translocation to the apical membrane (60). We have chosen to use phloridzin at 2 mM rather than higher concentrations to prevent the complete lack of sugar uptake, which on its own might hamper the energy-dependent process of apoptosis (16).

Glucose-mediated cytoprotective mechanisms have been reported in other cell types, e.g., myocytes, vascular smooth muscle cells, mast cells, and T cells. Hypoxia-induced apoptosis in myocytes is reduced by the presence of high glucose (18), and parallels the augmented expression of a glucose transporter, GLUT-4 (61). In vascular smooth muscle cells, balloon angioplasty injury induces cell apoptosis and enhances the expression of GLUT-1; overexpression of this glucose transporter reduces cell death after serum withdrawal and Fas ligand stimulation (19, 62). Drug-induced cell apoptosis in mast cells is associated with translocation of GLUT-1 onto the cell surface, and inhibition of glucose uptake increases the level of cell death (63). These studies together with the findings reported here indicate that a wide variety of stress stimuli, e.g., hypoxia, cytotoxic drugs, distension injury, and microbial products, may up-regulate the activity of glucose transporters. The present study demonstrates for the first time an active role for SGLT-1 in this process. Augmented glucose uptake may serve as a stress response leading to energy-dependent cytoprotection. Considering that the intestinal epithelium is the first line of defense against noxious luminal products, maintenance of barrier homeostasis is particularly significant. Further studies using alternative stressors, e.g., microbes, cytotoxic agents or immune factors, to

induce intestinal epithelial cell apoptosis *in vivo* are in progress to determine whether this glucose-mediated cytoprotective mechanism represents a generic response to any type of pathogenic proapoptotic stimulation in the intestine.

The mechanism of glucose-mediated cytoprotection was investigated. Intracellular levels of anti- and proapoptotic proteins belonging to the Bcl-2-related family may regulate cell survival. Western blot and densitometric analysis demonstrated reduced levels of anti-apoptotic Bcl-2, and unchanged levels of Bcl-X_L and Bax, in epithelial cells exposed to LPS in low glucose environments, consistent with the LPS-induced apoptosis. Presence of high glucose maintained the levels of Bcl-2 and increased anti-apoptotic Bcl-X_L, despite the presence of LPS. ELISA results further confirmed the reduction of total and phosphorylated anti-apoptotic Bcl-2 by LPS challenge in low glucose condition. Enhanced SGLT-1-mediated glucose uptake prevented the LPS-induced decrease of Bcl-2 levels, concurrently with the attenuation of cell death. Following our findings that LPS-induced apoptosis involved the reduction of mitochondrial membrane potential, changes in the expression of VDAC and the translocation of cytochrome *c* were also examined. LPS exposure induced the translocation of mitochondrial cytochrome *c* into the cytosol in low glucose media, but not in the presence of high glucose. Cytochrome *c* release is thought to occur via two possible routes, including the rupture of the outer mitochondrial membrane, and/or through specific channels formed by VDAC and/or other proapoptotic proteins, such as Bax (64). In the present study, negligible levels of VDAC were detected in the cytosolic

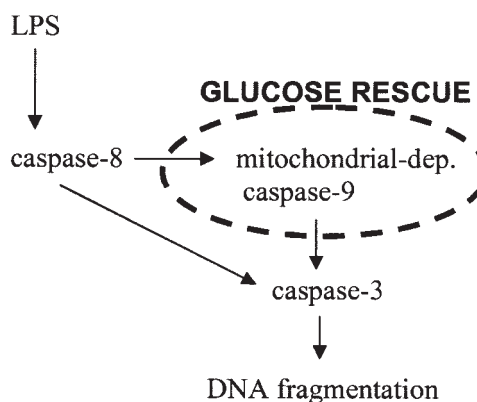


Figure 10. Schema of LPS-induced epithelial cell apoptosis and rescue pathway by high glucose. Our results show that LPS-induced apoptosis is dependent on caspase-8, -9, and -3, suggesting that LPS triggered both mitochondrial-dependent and -independent pathways. The finding that inhibitors of either caspase-8 or caspase-9 were able to completely abolish apoptosis triggered by LPS in low glucose conditions suggests the merging of the two pathways at one point, possibly by caspase-3. It is noteworthy that high glucose treatment was able to fully inhibit release of cytochrome *c* to cytosol, indicating that glucose rescues the mitochondrial pathway. Therefore, the mitochondrial-independent caspase-8 pathway may have contributed in part to the residual apoptotic levels detected after LPS challenge in high glucose conditions.

fractions of all groups, confirming the lack of mitochondrial contamination during sample preparation, but also suggesting that mitochondrial membrane rupture after LPS challenge was unlikely in this particular experimental setting. In contrast, the expression of mitochondrial membrane-bound VDAC increased after exposure to LPS in both low and high glucose media, suggesting downstream signaling by LPS, irrespective of the glucose concentration in the environment. This argues against the possibility that glucose modulates cell apoptosis by blocking LPS receptors, an important topic for further investigation. In addition, anti-apoptotic Bcl-2 and Bcl-X_L are known to block the opening of VDAC, and determine the gating capacity of this channel for cytochrome *c* release (14, 15). Electrophysiological studies using liposomes have shown that the interaction of Bax and VDAC forms pores that are permeable to cytochrome *c* (65). Conversely, Bcl-X_L inhibits VDAC activity and closes the channel by competing with Bax (65). Bcl-2 also inhibits Bax/Bak oligomerization in the mitochondrial membrane, an effect that further promotes VDAC-dependent or independent pore formation (66). The experiments described here found that the levels of Bax did not change after LPS treatment, while intracellular concentrations of Bcl-X_L were significantly elevated in LPS-treated cells under high glucose conditions. Together, these results suggest that enhanced expression of Bcl-X_L may have inhibited VDAC opening in the high glucose environment. The structural change induced by SGLT-1-mediated glucose uptake need to be characterized. The findings demonstrate that SGLT-1 mediates a glucose-dependent increase of Bcl-2 and Bcl-X_L, which in turn prevents the loss of mitochondrial membrane potential and the release of cytochrome *c*, and eventually, inhibit the process of apoptosis, such as that induced by LPS.

It is noteworthy that high glucose treatment was able to fully inhibit the release of cytochrome *c* to the cytosol induced by LPS, indicating that glucose rescues the mitochondrial pathway. However, high glucose reduced but did not eliminate apoptosis triggered by LPS. Our results indicate that LPS-induced apoptosis is dependent on caspase-8, -9, and -3, suggesting that LPS triggers both mitochondrial-dependent and -independent pathways. The finding that inhibitors of either caspase-8 or caspase-9 were able to completely abolish apoptosis triggered by LPS in low glucose conditions suggests the merging of the two pathways at one point, possibly by caspase-3 (Fig. 10). Therefore, the mitochondrial-independent caspase-8 pathway may have contributed in part to the residual apoptotic levels detected after LPS challenge in high glucose conditions.

Anti-apoptotic proteins, including poly(ADP-ribose) polymerization enzymes (PARP), FLICE-like apoptosis inhibitory protein (FLIP), and inhibitors of apoptosis proteins (IAPs), are important regulators of apoptotic cell death. PARP is activated after sensing of DNA damage, and repair DNA by synthesizing polymers of

ADP-ribose. During apoptosis, PARP is cleaved and inactivated by caspases to avoid DNA repair (67). Moreover, FLIP competes with caspase 8 for binding to FADD, and plays a role in the protection of endothelial cells from LPS-induced apoptosis and the suppression of NFκB activation (68). Whether these anti-apoptotic proteins are also implicated in the glucose-mediated rescue of intestinal epithelial cells remains obscure.

A recent study has found that inhibition of glucose metabolism sensitizes tumor cell to death receptor-triggered apoptosis, via changes in cFLIP levels and early processing of pro-caspase-8. The use of glucose deprivation was implied as an important target for cancer therapy (69). This observation provides additional support to our hypothesis that increased glucose uptake may attenuate cell apoptosis triggered by pro-apoptotic stimuli, such as LPS in the present study. Clearly, in the context of maintaining homeostasis, desensitization to proapoptotic stimuli is beneficial to maintain normal function in healthy epithelia, but would be detrimental to the host when affecting tumor cells. Our findings that increased glucose concentrations do not inhibit the baseline level of cell apoptosis (Fig. 1A–C), provide evidence that glucose per se does not promote tumorigenesis.

In summary, findings from this study demonstrate that SGLT-1-mediated glucose uptake protects intestinal epithelial cells against LPS-induced apoptosis and barrier defects. Mechanisms involved include the up-regulation of Bcl-2 and Bcl-X_L, and inhibition of the translocation of cytochrome *c*. The study presents a novel rescue mechanism against enterocyte apoptosis. The understanding of this cytoprotective mechanism has physiological and pathological implications that may provide insights into the development of novel therapeutic interventions to correct excessive pathological cell death and increased paracellular permeability in a variety of intestinal diseases, including IBD and bacterial enteritis. FJ

Funded by CAG/CIHR/NSERC/AstraZeneca.

REFERENCES

1. Madara, J. L. (1990) Maintenance of the macromolecular barrier at cell extrusion sites in intestinal epithelium: physiological rearrangement of tight junctions. *J. Membr. Biol.* **116**, 177–184
2. Scott, K. G., Meddings, J. B., Kirk, D. R., Lees-Miller, S. P., and Buret, A. G. (2002) Intestinal infection with *Giardia* spp. reduces epithelial barrier function in a myosin light chain kinase-dependent fashion. *Gastroenterology* **123**, 1179–1190
3. Chin, A. C., Teoh, D. A., Scott, K. G., Meddings, J. B., MacNaughton, W. K., and Buret, A. G. (2002) Strain-dependent induction of enterocyte apoptosis by *Giardia lamblia* disrupts epithelial barrier function in a caspase-3-dependent manner. *Infect. Immun.* **70**, 3673–3680
4. Jones, N. L., Iskur, A., Haq, R., Mascarenhas, M., Karmali, M. A., Perdue, M. H., Zanke, B. W., and Sherman, P. M. (2000) *Escherichia coli* Shiga toxins induce apoptosis in epithelial cells that is regulated by the Bcl-2 family. *Am. J. Physiol.* **278**, G811–G819

5. Paesold, G., Guiney, D. G., Eckmann, L., and Kagnoff, M. F. (2002) Genes in the Salmonella pathogenicity island 2 and the Salmonella virulence plasmid are essential for Salmonella-induced apoptosis in intestinal epithelial cells. *Cell. Microbiol.* **4**, 771–781
6. Le'Negrato, G., Ricci, V., Hofman, V., Mograbi, B., Hofman, P., and Rossi, B. (2001) Epithelial intestinal cell apoptosis induced by *Helicobacter pylori* depends on expression of the cag pathogenicity island phenotype. *Infect. Immun.* **69**, 5001–5009
7. Giovannini, C., Matarrese, P., Scazzocchio, B., Vari, R., D'Archivio, M., Straface, E., Masella, R., Malorni, W., and De Vincenzi, M. (2003) Wheat gliadin induces apoptosis of intestinal cells via an autocrine mechanism involving Fas-Fas ligand pathway. *FEBS Lett.* **540**, 117–124
8. Deng, W., Balazs, L., Wang, D. A., Van Middlesworth, L., Tigyi, G., and Johnson, L. R. (2002) Lysophosphatidic acid protects and rescues intestinal epithelial cells from radiation- and chemotherapy-induced apoptosis. *Gastroenterology* **123**, 206–216
9. Gitter, A. H., Bendfeldt, K., Schulzke, J. D., and Fromm, M. (2000) Leaks in the epithelial barrier caused by spontaneous and TNF-alpha-induced single-cell apoptosis. *FASEB J.* **14**, 1749–1753
10. Abreu, M. T., Palladino, A. A., Arnold, E. T., Kwon, R. S., and McRoberts, J. A. (2000) Modulation of barrier function during Fas-mediated apoptosis in human intestinal epithelial cells. *Gastroenterology* **119**, 1524–1536
11. Merger, M., Viney, J. L., Borojevic, R., Steele-Norwood, D., Zhou, P., Clark, D. A., Riddell, R., Maric, R., Podack, E. R., and Croitoru, K. (2002) Defining the roles of perforin, Fas/FasL, and tumour necrosis factor alpha in T cell induced mucosal damage in the mouse intestine. *Gut* **51**, 155–163
12. Ramachandran, A., Madesh, M., and Balasubramanian, K. A. (2000) Apoptosis in the intestinal epithelium: its relevance in normal and pathophysiological conditions. *J. Gastroenterol. Hepatol.* **15**, 109–120
13. Mayer, B., and Oberbauer, R. (2003) Mitochondrial regulation of apoptosis. *News Physiol. Sci.* **18**, 89–94
14. Shimizu, S., Narita, M., and Tsujimoto, Y. (1999) Bcl-2 family proteins regulate the release of apoptogenic cytochrome *c* by the mitochondrial channel VDAC. *Nature (London)* **399**, 483–487
15. Zheng, Y., Shi, Y., Tian, C., Jiang, C., Jin, H., Chen, J., Almasan, A., Tang, H., and Chen, Q. (2004) Essential role of the voltage-dependent anion channel (VDAC) in mitochondrial permeability transition pore opening and cytochrome *c* release induced by arsenic trioxide. *Oncogene* **23**, 1239–1247
16. Eguchi, Y., Shimizu, S., and Tsujimoto, Y. (1997) Intracellular ATP levels determine cell death fate by apoptosis or necrosis. *Cancer Res.* **57**, 1835–1840
17. Thakkar, N. S., and Potten, C. S. (1993) Inhibition of doxorubicin-induced apoptosis in vivo by 2-deoxy-D-glucose. *Cancer Res.* **53**, 2057–2060
18. Schaffer, S. W., Croft, C. B., and Solodushko, V. (2000) Cardio-protective effect of chronic hyperglycemia: effect on hypoxia-induced apoptosis and necrosis. *Am. J. Physiol.* **278**, H1948–H1954
19. Hall, J. L., Chatham, J. C., Eldar-Finkelman, H., and Gibbons, G. H. (2001) Upregulation of glucose metabolism during intimal lesion formation is coupled to the inhibition of vascular smooth muscle cell apoptosis. Role of GSK3beta. *Diabetes* **50**, 1171–1179
20. Malhotra, R., Lin, Z., Vincenz, C., and Brosius, F. C., III (2001) Hypoxia induces apoptosis via two independent pathways in Jurkat cells: differential regulation by glucose. *Am. J. Physiol.* **281**, C1596–C1603
21. Hediger, M. A., Coady, M. J., Ikeda, T. S., and Wright, E. M. (1987) Expression cloning and cDNA sequencing of the Na⁺/glucose co-transporter. *Nature (London)* **330**, 379–381
22. Scheepers, A., Joost, H. G., and Schurmann, A. (2004) The glucose transporter families SGLT and GLUT: molecular basis of normal and aberrant function. *JPEN J. Parenter. Enteral Nutr.* **28**, 364–371
23. Kimmich, G. A., and Randles, J. (1981) alpha-Methylglucoside satisfies only Na⁺-dependent transport system of intestinal epithelium. *Am. J. Physiol.* **241**, C227–C232
24. Kimmich, G. A., and Randles, J. (1984) Sodium-sugar coupling stoichiometry in chick intestinal cells. *Am. J. Physiol.* **247**, C74–C82
25. Darfeuille-Michaud, A., Neut, C., Barnich, N., Lederman, E., Di Martino, P., Desreumaux, P., Gambiez, L., Joly, B., Cortot, A., and Colombel, J. F. (1998) Presence of adherent *Escherichia coli* strains in ileal mucosa of patients with Crohn's disease. *Gastroenterology* **115**, 1405–1413
26. Neut, C., Bulois, P., Desreumaux, P., Membre, J. M., Lederman, E., Gambiez, L., Cortot, A., Quandalle, P., van Kruiningen, H., and Colombel, J. F. (2002) Changes in the bacterial flora of the neoterminal ileum after ileocolonic resection for Crohn's disease. *Am. J. Gastroenterol.* **97**, 939–946
27. Cario, E., Rosenberg, I. M., Brandwein, S. L., Beck, P. L., Reinecker, H. C., and Podolsky, D. K. (2000) Lipopolysaccharide activates distinct signaling pathways in intestinal epithelial cell lines expressing Toll-like receptors. *J. Immunol.* **164**, 966–972
28. Bocker, U., Schottelius, A., Watson, J. M., Holt, L., Licato, L. L., Brenner, D. A., Sartor, R. B., and Jobin, C. (2000) Cellular differentiation causes a selective down-regulation of interleukin (IL)-1beta-mediated NF-kappaB activation and IL-8 gene expression in intestinal epithelial cells. *J. Biol. Chem.* **275**, 12207–12213
29. Cario, E., and Podolsky, D. K. (2000) Differential alteration in intestinal epithelial cell expression of toll-like receptor 3 (TLR3) and TLR4 in inflammatory bowel disease. *Infect. Immun.* **68**, 7010–7017
30. Gardiner, K. R., Halliday, M. I., Barclay, G. R., Milne, L., Brown, D., Stephens, S., Maxwell, R. J., and Rowlands, B. J. (1995) Significance of systemic endotoxaemia in inflammatory bowel disease. *Gut* **36**, 897–901
31. Caradonna, L., Amati, L., Magrone, T., Pellegrino, N. M., Jirillo, E., and Caccavo, D. (2000) Enteric bacteria, lipopolysaccharides and related cytokines in inflammatory bowel disease: biological and clinical significance. *J. Endotoxin Res.* **6**, 205–214
32. Turner, J. R., Lencer, W. I., Carlson, S., and Madara, J. L. (1996) Carboxy-terminal vesicular stomatitis virus G protein-tagged intestinal Na⁺-dependent glucose cotransporter (SGLT1): maintenance of surface expression and global transport function with selective perturbation of transport kinetics and polarized expression. *J. Biol. Chem.* **271**, 7738–7744
33. Marchetti, P., Castedo, M., Susin, S. A., Zamzami, N., Hirsch, T., Macho, A., Haeflner, A., Hirsch, F., Geuskens, M., and Kroemer, G. (1996) Mitochondrial permeability transition is a central coordinating event of apoptosis. *J. Exp. Med.* **184**, 1155–1160
34. Chin, A. C., Vergnolle, N., MacNaughton, W. K., Wallace, J. L., Hollenberg, M. D., and Buret, A. G. (2003) Proteinase-activated receptor 1 activation induces epithelial apoptosis and increases intestinal permeability. *Proc. Natl. Acad. Sci. USA* **100**, 11104–11109
35. Rao, J. N., Guo, X., Liu, L., Zou, T., Murthy, K. S., Yuan, J. X., and Wang, J. Y. (2003) Polyamines regulate Rho-kinase and myosin phosphorylation during intestinal epithelial restitution. *Am. J. Physiol.* **284**, C848–C859
36. Saikumar, P., Dong, Z., Patel, Y., Hall, K., Hopfer, U., Weinberg, J. M., and Venkatachalam, M. A. (1998) Role of hypoxia-induced Bax translocation and cytochrome *c* release in reoxygenation injury. *Oncogene* **17**, 3401–3415
37. Turner, J. R., Rill, B. K., Carlson, S. L., Carnes, D., Kerner, R., Mrsny, R. J., and Madara, J. L. (1997) Physiological regulation of epithelial tight junctions is associated with myosin light-chain phosphorylation. *Am. J. Physiol.* **273**, C1378–C1385
38. Madara, J. L., Moore, R., and Carlson, S. (1987) Alteration of intestinal tight junction structure and permeability by cytoskeletal contraction. *Am. J. Physiol.* **253**, C854–C861
39. Amano, M., Ito, M., Kimura, K., Fukata, Y., Chihara, K., Nakano, T., Matsuura, Y., and Kaibuchi, K. (1996) Phosphorylation and activation of myosin by Rho-associated kinase (Rho-kinase). *J. Biol. Chem.* **271**, 20246–20249
40. Berglund, J. J., Riegler, M., Zolotarevsky, Y., Wenzl, E., and Turner, J. R. (2001) Regulation of human jejunal transmucosal resistance and MLC phosphorylation by Na⁽⁺⁾-glucose cotransport. *Am. J. Physiol.* **281**, G1487–G1493
41. Yagi, S., Takaki, A., Hori, T., and Sugimura, K. (2002) Enteric lipopolysaccharide raises plasma IL-6 levels in the hepatoportal vein during noninflammatory stress in the rat. *Fukuoka Acta Med* **93**, 38–52
42. Drewe, J., Beglinger, C., and Fricker, G. (2001) Effect of ischemia on intestinal permeability of lipopolysaccharide. *Eur. J. Clin. Invest.* **31**, 138–144
43. Yamada, T., Inui, A., Hayashi, N., Fujimura, M., and Fujimiya, M. (2003) Serotonin stimulates endotoxin translocation via 5-HT3 receptors in the rat ileum. *Am. J. Physiol.* **284**, G782–G788

44. Imaeda, H., Yamamoto, H., Takaki, A., and Fujimiya, M. (2002) In vivo response of neutrophils and epithelial cells to lipopolysaccharide injected into the monkey ileum. *Histochem. Cell Biol.* **118**, 381–388
45. Courtois, F., Seidman, E. G., Delvin, D., Asselin, C., Bernotti, S., Ledoux, M., and Levy, E. (2003) Membrane peroxidation by lipopolysaccharide and iron-ascorbate adversely affects Caco-2 cell function: beneficial role of butyric acid. *Am. J. Clin. Nutr.* **77**, 744–750
46. Unno, N., Wang, H., Menconi, M. J., Tytgat, S. H., Larkin, V., Smith, M., Morin, M. J., Chavez, A., Hodin, R. A., and Fink, M. P. (1997) Inhibition of inducible nitric oxide synthase ameliorates endotoxin-induced gut mucosal barrier dysfunction in rats. *Gastroenterology* **113**, 1246–1257
47. Eckmann, L., Jung, H. C., Schurer-Maly, C., Panja, A., Morzycka-Wroblewska, E., and Kagnoff, M. F. (1993) Differential cytokine expression by human intestinal epithelial cell lines: regulated expression of interleukin 8. *Gastroenterology* **105**, 1689–1697
48. Eipel, C., Bordel, R., Nickels, R. M., Menger, M. D., and Vollmar, B. (2004) Impact of leukocytes and platelets in mediating hepatocyte apoptosis in a rat model of systemic endotoxemia. *Am. J. Physiol.* **286**, G769–G776
49. Schildberg, F. A., Schulz, S., Dombrowski, F., and Minor, T. (2005) Cyclic AMP alleviates endoplasmic stress and programmed cell death induced by lipopolysaccharides in human endothelial cells. *Cell Tissue Res.*
50. Rudkowski, J. C., Barreiro, E., Harfouche, R., Goldberg, P., Kishta, O., D'Orleans-Juste, P., Labonte, J., Lesur, O., and Hussain, S. N. (2004) Roles of iNOS and nNOS in sepsis-induced pulmonary apoptosis. *Am. J. Physiol.* **286**, L793–L800
51. Ortiz-Arduan, A., Danoff, T. M., Kalluri, R., Gonzalez-Cuadrado, S., Karp, S. L., Elkon, K., Egado, J., and Neilson, E. G. (1996) Regulation of Fas and Fas ligand expression in cultured murine renal cells and in the kidney during endotoxemia. *Am. J. Physiol.* **271**, F1193–F1201
52. Antonelli, A., Bianchi, M., Crinelli, R., Gentilini, L., and Maggani, M. (2001) Modulation of ICAM-1 expression in ECV304 cells by macrophage-released cytokines. *Blood Cells Mol. Dis.* **27**, 978–991
53. Power, C., Wang, J. H., Sookhai, S., Street, J. T., and Redmond, H. P. (2001) Bacterial wall products induce downregulation of vascular endothelial growth factor receptors on endothelial cells via a CD14-dependent mechanism: implications for surgical wound healing. *J. Surg. Res.* **101**, 138–145
54. Regoli, D. C., Marceau, F., and Lavigne, J. (1981) Induction of beta-1-receptors for kinins in the rabbit by a bacterial lipopolysaccharide. *Eur. J. Pharmacol.* **71**, 105–115
55. Sato, N., Takahashi, N., Suda, K., Nakamura, M., Yamaki, M., Ninomiya, T., Kobayashi, Y., Takada, H., Shibata, K., Yamamoto, M., et al. (2004) MyD88 but not TRIF is essential for osteoclastogenesis induced by lipopolysaccharide, diacyl lipopeptide, and IL-1alpha. *J. Exp. Med.* **200**, 601–611
56. Rosenblatt, J., Raff, M. C., and Cramer, L. P. (2001) An epithelial cell destined for apoptosis signals its neighbors to extrude it by an actin- and myosin-dependent mechanism. *Curr. Biol.* **11**, 1847–1857
57. Nazli, A., Yang, P. C., Jury, J., Howe, K., Watson, J. L., Soderholm, J. D., Sherman, P. M., Perdue, M. H., and McKay, D. M. (2004) Epithelia under metabolic stress perceive commensal bacteria as a threat. *Am. J. Pathol.* **164**, 947–957
58. Bojarski, C., Weiske, J., Schoneberg, T., Schroder, W., Mankertz, J., Schulzke, J. D., Florian, P., Fromm, M., Tauber, R., and Huber, O. (2004) The specific fates of tight junction proteins in apoptotic epithelial cells. *J. Cell Sci.* **117**, 2097–2107
59. Han, X., Fink, M. P., Yang, R., and Delude, R. L. (2004) Increased iNOS activity is essential for intestinal epithelial tight junction dysfunction in endotoxemic mice. *Shock* **21**, 261–270
60. Kellett, G. L. (2001) The facilitated component of intestinal glucose absorption. *J. Physiol.* **531**, 585–595
61. Sun, D., Nguyen, N., DeGrado, T. R., Schwaiger, M., and Brosius, F. C., III (1994) Ischemia induces translocation of the insulin-responsive glucose transporter GLUT4 to the plasma membrane of cardiac myocytes. *Circulation* **89**, 793–798
62. Pollman, M. J., Hall, J. L., and Gibbons, G. H. (1999) Determinants of vascular smooth muscle cell apoptosis after balloon angioplasty injury. Influence of redox state and cell phenotype. *Circ. Res.* **84**, 113–121
63. Kan, O., Baldwin, S. A., and Whetton, A. D. (1994) Apoptosis is regulated by the rate of glucose transport in an interleukin 3 dependent cell line. *J. Exp. Med.* **180**, 917–923
64. Tsujimoto, Y., and Shimizu, S. (2000) VDAC regulation by the Bcl-2 family of proteins. *Cell Death Differ.* **7**, 1174–1181
65. Shimizu, S., Ide, T., Yanagida, T., and Tsujimoto, Y. (2000) Electrophysiological study of a novel large pore formed by Bax and the voltage-dependent anion channel that is permeable to cytochrome c. *J. Biol. Chem.* **275**, 12321–12325
66. Yi, X., Yin, X. M., and Dong, Z. (2003) Inhibition of Bid-induced apoptosis by Bcl-2, tBid insertion, Bax translocation, and Bax/Bak oligomerization suppressed. *J. Biol. Chem.* **278**, 16992–16999
67. Ivana, S. A., and Diederich, M. (2004) Modulation of poly(ADP-ribosylation) in apoptotic cells. *Biochem. Pharmacol.* **68**, 1041–1047
68. Bannerman, D. D., Eiting, K. T., Winn, R. K., and Harlan, J. M. (2004) FLICE-like inhibitory protein (FLIP) protects against apoptosis and suppresses NF-kappaB activation induced by bacterial lipopolysaccharide. *Am. J. Pathol.* **165**, 1423–1431
69. Munoz-Pinedo, C., Ruiz-Ruiz, C., Ruiz de Almodovars, C., Palacios, C., and Lopez-Rivas, A. (2003) Inhibition of glucose metabolism sensitizes tumor cells to death receptor-triggered apoptosis through enhancement of death-inducing signaling complex formation and apical procaspase-8 processing. *J. Biol. Chem.* **278**, 12759–12768

Received for publication April 27, 2005.
Accepted for publication July 25, 2005.